Synchronous Reference Frame Control of Transformer Based DC mA Current Sensor

Muhammed Calar
Defense System Technologies
Aselsan Inc, Gazi University
Ankara, Turkey
muhammedcalar20041999@gmail.com

Korhan Kayisli
Electrical and Electronics Engineering Dept.
Gazi University
Ankara, Turkey
korhankayisli@gazi.edu.tr

***Abstract*— This paper addresses the measurement of DC current with a transformer by the second harmonic detection method which uses the principle of the fluxgate magnetometer. The DC current passing through the high-susceptibility, saturated ferromagnetic metal core is observed. Changes in the DC current create a difference in the harmonics of the sense winding of the current transformer. The sensor's sense winding signals and its harmonic components have been observed at different values of the current. In order to find the exact current value, a Synchronous Reference Frame (SRF) control method has been applied. By applying the proposed Synchronous Reference Frame (SRF) control method to the sensor's secondary winding signal, second harmonic value is obtained. The change at the second harmonic is used to obtain the current. Compensation current is applied in the reverse direction to the measured current, to increase the sustainability of the current sensor.**

Keywords*— *Current sensor, DC transformer, Direct current current sensor (DCCT), Synchronous Reference Frame (SRF)

I. INTRODUCTION

With the rapid development of power electronic devices, the requirement of measurement systems needed by converters, machine drives, and electrical machines has increased such as voltage and current measurements [1]. Current measurements play an important role in increasing the controllability and protection of smart grid applications. For these major applications, the requirement for current sensors has increased [2]. There are a number of current measurement methods based on Faraday's Law exist in literature such as Current transformer (CT), and Rogowski coil. Also, current sensors that are based on the magnetic field are Hall effect, Fluxgate sensors, and magneto-resistive current sensors have been developed. There are some studies were presented about detecting and measuring the current electromagnetically such as, minimizing power consumption by using the ferro resonance feature [3], using a transformer to measure currents with small values, detecting current at the secondary winding where it acts in linear behavior [4], a transformer with high linearity and Faraday's law based on high precision, current measurement with electromagnetic effect [5], current measurement using transformers for digitally controlled power supplies [6], use of transformers for current measurements in power networks [7], current measurement in PWM converters, with using transformers at similar structure [8].

In most CT applications ferrite toroid core is used. It relies on Faraday's law and if a coil is placed in a changing electromagnetic field a force occurs in that coil. Since the coil is placed in changing electromagnetic field, DC values cannot be measured by this method. In order to measure DC, DC current transformer (DCCT), shown in Fig. 1 was introduced by Unser at CERN (European Organization for Nuclear Research) in 1966 [9]. It consists of two identical ferrite toroidal cores which get saturated by AC current signals. When current flow through the given cores, its DC level will introduce an asymmetry and give an output consisting of even harmonics of the modulation frequency [10]. To detect the amplitude of the harmonic, a demodulator is used. Compensating current decided by the demodulator is applied to the system in order to make the total magnetic flux to the initial state which is called the zero-flux principle.

There are many different approaches for the current measurement of high-accuracy DC. Generally, the detection characteristics of the current sensors are usually depending on the magnetic features and geometric design of the core [11].

In a study on magnetic field-controlled current sensor based on zero magnetic field, for current measurement, a current is applied in the reverse direction of the measured current to make the balancing magnetic force to its initial value. Then, the measured current value is obtained from the applied current value. The triangular wave current excitation method is applied to find the zero state of the current sensor in the given approach. For this triangular wave current method, when the magnetization current is zero, it appears symmetrical on the both negative and positive sides. When the core is magnetized by a current, it can be detected by the change between the negative and positive sides [11].

In another research, DC measuring is combined with a second harmonic modulator and a CT [12]. The combined CT consists of a number of toroidal cores, which have high permeability Ni-Fe alloy [12]. It also uses a modulator that has an excitation current of constant value at 250Hz and a demodulator that has a 500Hz value of phase reference signal. Modulator pairs are identically excited but they are wounded in opposite directions. The output signal voltage is proportional to the beam current and it is deduced from the current flow in the shunt resistor at the output. The demodulator is detecting the phase and amplitude of the second harmonic at the signal output of the modulator cores.

Perfect beam current monitors should have a high resolution and provide an output proportional to the beam current [13]. The beam CT is most likely the best solution but it has some shortcomings which are, limited operating frequency range and lack of sensitivity [13]. The core losses in CT are mainly caused by eddy currents. In a properly

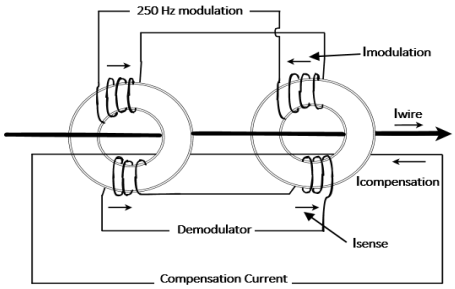

Fig. 1 The structure of Classical DC Current Transformer (DCCT)

designed current sensor, this loss should be very small or neglected. For a fast passive CT working with high frequency, stray capacitance and leakage inductance of the secondary winding are kept at a minimum, and a tape wound core with minimum tape thickness is used [13]. In this approach, a magnetic modulator is added to the active-passive CT in order to measure DC.

In this study, in order to measure DC current without any loss, a sensor that can measure DC with two toroid cores is designed. The prototype design and capability of the sensor are mentioned. The value of the measured current can be obtained by operating a saturable transformer in a non-linear region, and park transformation applied to the signal induced from the secondary winding. The second and multiple harmonics of the sensed signal change with the magnitude of the current. By detecting the magnitude of the harmonic, the current value can be calculated [14,15]. In this work, the second harmonic of the sensed signal on the secondary winding is used for measurements. DCCT is used with Texas Instruments TMS320F2837D microcontroller. The output of the microcontroller is used for the core saturation and producing compensation current in the reverse direction to decrease the second harmonic value of the sensed secondary winding signal to its initial value. The analog inputs of the microcontroller are used to detect secondary winding voltage, and park transformation is applied to the detected signal and its 90 degrees delayed forms. By this control method, the magnitude of the second harmonic can be detected. Change in the second harmonic of the current provides the magnitude of the current that passes through the core. This current measurement method gives precise current detection.

II. Synchronous Reference Frame (SRF) Method

A synchronous Reference Frame (SRF) can be used to detect the harmonics of the voltages or currents [16]. SRF method is based on the a-b-c to d-q transformation which is a sequence of Clark and Park transformation. Alternating signals can be shown as vectors rotating with an angular velocity of its angular frequency on a Cartesian coordinate reference frame [17]. The magnitude of the vectors gives the peak value of the associated signal phases. Since an observer on a stationary reference frame is observing alternating signal vector representations, it is demonstrated that they are spinning with an angular velocity. Assume that the reference frame is also spinning, either clockwise or counterclockwise, with any angular velocity. In this scenario, the relative angular velocities of the alternating signal vectors with respect to rotating reference frames should be used to describe the signal vectors. The term "SRF" refers to a reference frame that is selected to spin at precisely the same

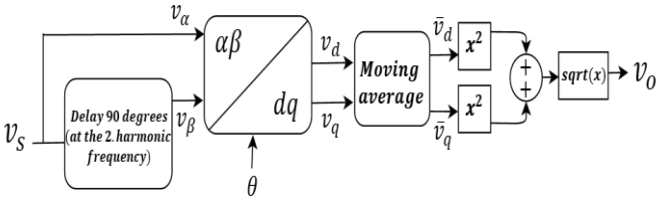

Fig. 2 SRF Control Method

angular velocity as the alternating signal.

In this study, harmonic content was derived by utilizing the SRF approach. To derive the harmonics, an SRF rotating synchronously with the fundamental frequency of the load current signal should be created. The Clarke and Park transformations and two sequential transformation processes are necessary for transformation. First, using the Clarke Transformation given in (1), three-phase signal vectors can be transformed into perpendicular two-phase representation, namely phase (alpha) and (beta).

$$\begin{bmatrix} i_0 \\ i_\alpha \\ i_\beta \end{bmatrix} = \sqrt{\frac{2}{3}} \begin{bmatrix} \frac{1}{\sqrt{2}} & \frac{1}{\sqrt{2}} & \frac{1}{\sqrt{2}} \\ 1 & -\frac{1}{2} & -\frac{1}{2} \\ 0 & \frac{\sqrt{3}}{2} & -\frac{\sqrt{3}}{2} \end{bmatrix} \begin{bmatrix} i_a \\ i_b \\ i_c \end{bmatrix} \quad (1)$$

Following the use of Clarke transformation, Park transformation can be used to transform the two-phase representation of the signals into the direct (d) and quadrature (q) axes of the SRF. The Park transformation given in (2) is used to determine the projections of the alpha and beta phases on the d and q axes of the SRF.

$$\begin{bmatrix} i_d \\ i_q \end{bmatrix} = \begin{bmatrix} cos(\theta) & sin(\theta) \\ -sin(\theta) & cos(\theta) \end{bmatrix} \begin{bmatrix} i_\alpha \\ i_\beta \end{bmatrix} \quad (2)$$

The block diagram for the calculation of the second harmonic of the secondary winding signal, SRF method is illustrated in Fig. 2. Instantaneous values of secondary winding signals are transformed to a d-q reference frame via a combination of Clarke and Park transformations.

III. Sensor Design

Classical DCCT operation is studied in this paper. Two identical Magnetics products with the part number ZW44920TC ferrite toroidal cores are used in the experiment. The excitation windings of the cores are wounded up-reverse, and modulation current which is 250Hz, 10.85A is applied to the cores. The modulation signal is a 250Hz sinusoidal wave and the magnitude of the signal is enough to drive both cores to work in saturation. Thus, saturating the cores will create a signal on sense winding. A primary DC current that flows through the sensor shifts the cores' working point in opposite polarity [17]. It generates a second harmonic of the modular frequency. The signal obtained from sense winding is given to the TMS320F2837D's ADC pins and the SRF method is applied to detect the second harmonic. The current that passes through the cores changes the magnitude of the second harmonic of the sensed signal and it is proportional to the current passing through the cores. SRF method is applied to the sensed signal to detect the second harmonic which occurs

TABLE I. Parameters of the used ferrite cores

Parameter	**Value**
Outer Diameter (mm)	47.6
Inner Diameter (mm)	30.27
Height (mm)	15.55
Permeability (μ)	10000

at 500Hz. Since the 250Hz saturation current is applied to saturate cores, harmonics at 500 Hz are observed. The compensation current is applied in the reverse direction to cancel the magnetic flux to zero state. The second harmonic is calculated and the error value is generated from the conversion. The error is applied to the cores in, the reverse direction to the measured current. Applied reverse current will cancel the magnetic flux and make the error value zero. The increase or decrease in the measured current changes the second harmonic magnitude which changes the error value. At last, this error is given to the Proportional Integral (PI) controller, and compensation current is applied with the changes at the error value. PI parameters are obtained manually. First, the integral gain is set to zero, then the proportional gain is increased slowly until oscillation occurs at the output of the controller. The proportional gain is set to 10 and then the integral gain is increased slowly until any offset is corrected for on the timescale that is appropriate for the control system and integral the gain is set to 0.012. Parameters of the used ferrite cores are given in TABLE I.

The measured signal from the sense winding is given in Fig. 3, and Fig. 7, and the SRF method is applied to the sense winding signal and its 90 degrees delayed form to calculate the second harmonic occurs at 500 Hz, and the change in the magnitude of the second harmonic is given as error. This error is eliminated with the compensation current which is applied reverse to the measured current.

IV. Experimental Results

Two identical ferrite toroid cores are saturated at 10.85A and 5.55A values. The sensed signal in the secondary winding (sense winding) is taken at 0 mA and 100 mA values and given in Fig. 3, and Fig. 7. Increasing the current passing through the core increase the magnitude of the sense winding signal in the secondary winding of the saturated core. DC current and output compensation currents are given in TABLE II and TABLE III. The error value is calculated from the difference between these currents and given in TABLE II and TABLE III. Second harmonic values are taken at 500Hz. Since cores are saturated at 250Hz second harmonics are taken at 500Hz. It was observed from the obtained data in TABLE II and TABLE III that the second harmonic of the sense winding signal is proportional to the measured current. After applying the compensation current reverse to the measured current, the magnitude of the second harmonic is decreased to its zero-flux state. It can be seen from TABLE II and TABLE III that saturating cores at high currents decrease the difference in the magnitude of the second harmonic at different values of the current. Comparing the second harmonic value for both saturations, second harmonic value changes more for a 5.55A saturation. For better resolution, cores should be saturated at lower current values.

CT saturated with 10.85A-250Hz and park transformation is applied to the sense winding signal. Harmonics of sense winding signal illustrated in Fig. 3. Harmonics are taken at

TABLE II Results for 10.85A saturated sensor

Current (mA)	Second Harmonic without compensation current applied (mV)	Compensation current (mA)	Error (%)
0	0.087	0	-
10	1.2	10.10	1
20	2.4	19.81	0.95
30	3.6	29.1	3
40	4.8	38.9	2.75
50	5.9	48.8	2.4
60	7.0	58.5	2.5
70	8.1	69	1.42
80	9.2	79.4	0.75
90	10.3	89.5	0.55
100	11.4	99	1

TABLE III Results for 5.55A saturated sensor

Current (mA)	Second Harmonic without compensation current applied (mV)	Compensation current (mA)	Error (%)
0	0.025	0	-
10	1.32	10	-
20	2.72	19.5	2.5
30	4.13	29	3.3
40	5.56	39	2.5
50	6.95	48	4
60	8.35	58	3.3
70	9.71	68	2.8
80	11.00	78	2.5
90	12.32	89	1.1
100	13.60	98	2

measured current's 0mA and 100mA values. Second and multiple harmonics of the sense winding signal is given in Fig. 4 for the measured currents at 0mA and 100mA values. The change in second and multiple harmonics of the sense winding signal is observed. By applying the park transformation to the sense winding signal and its 90 degrees delayed form, second harmonic obtained at different measured current values and given in TABLE II. At 0mA second harmonic of the sense winding signal was 0.087mV and at 100mA second harmonic of the sense winding signal was 11.4mV.

CT saturated with 5.55A-250Hz and park transformation is applied to the sense winding signal. Harmonics of sense winding signal illustrated in Fig. 7. Harmonics are taken at measured current's 0mA and 100mA values. Second and multiple harmonics of the sense winding signal is given in Fig. 8 for measured current's 0mA and 100mA values. The change in second and multiple harmonics of the sense winding signal is observed. By applying the park transformation to the sense winding signal and its 90 degrees delayed form, second harmonic obtained at different measured current values and given in TABLE III. At 0mA second harmonic of the sense winding signal was 25μV and at 100mA second harmonic of the sense winding signal was 13.6mV.

Difference in the second harmonics at different current values was much more for the 5.55A saturated sensor. By calculating the difference in the second harmonic measured current is observed and the error value of the system is given to the PI system. The PI system is used for decrease the second harmonic to its 0mA value. Second harmonic of the sense winding signal is decreased to its initial zero- flux value by applying the compensation current in reverse direction of the measured current. Applying the compensation current in reverse to the measured current makes the current sensor more sustainable.

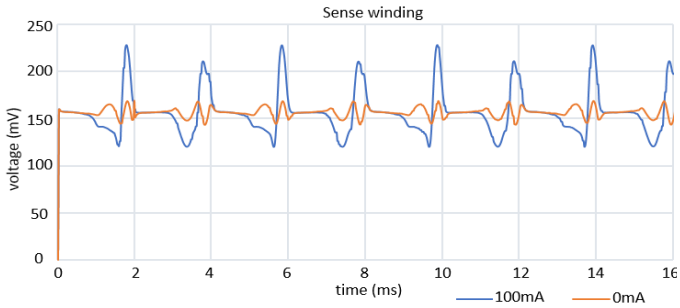

Fig. 3 Sensed signals at 10.85 A saturation

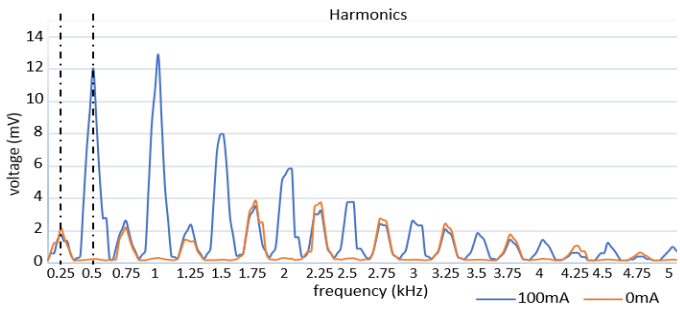

Fig. 4 Harmonic values at 10.85 A saturation

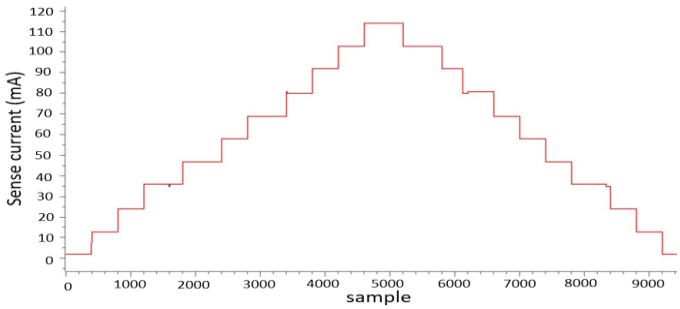

Fig. 5 Increasing current 10mA steps at 10.85 A saturation

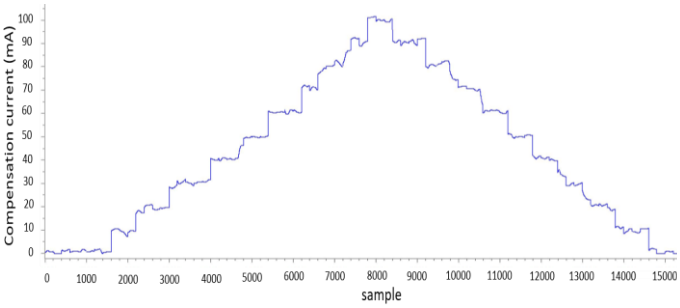

Fig. 6 Compensation currents increasing current 10mA steps at 10.85 A saturation

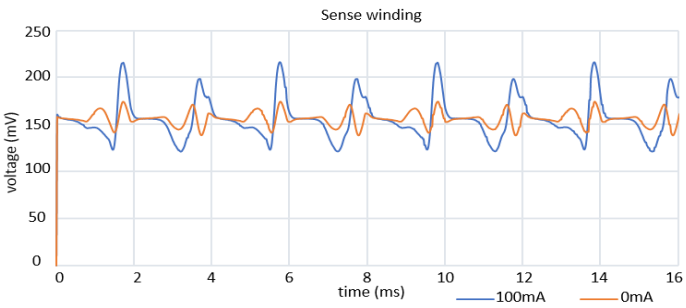

Fig. 7 Sensed signals at 5.55 A saturation

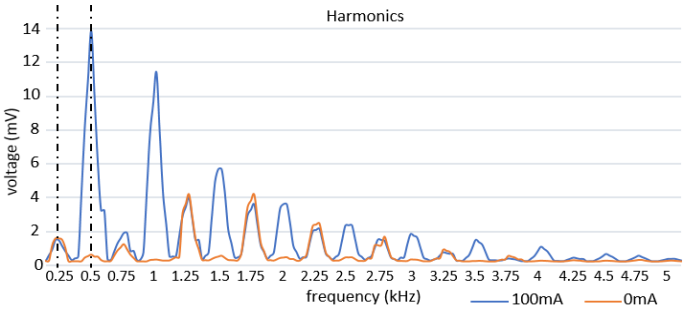

Fig. 8 Harmonic values at 5.55 A saturation

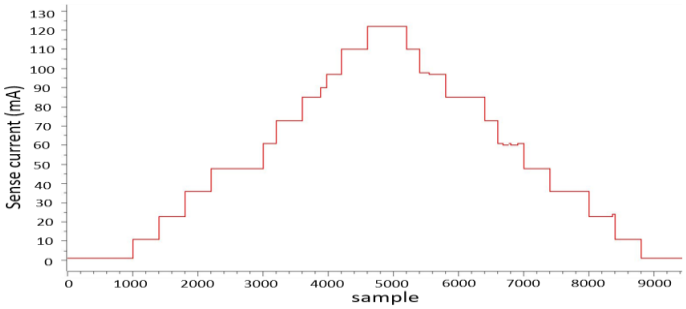

Fig. 9 Increasing current 10mA steps at 5.55 A saturation

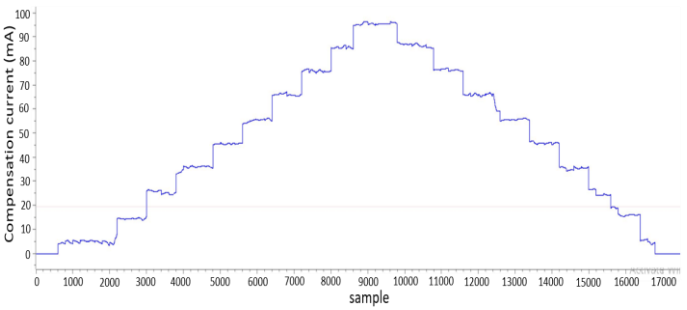

Fig. 10 Compensation currents increasing current 10mA steps at 5.55 A saturation

TABLE IV Performance parameters of the current sensor

Current range (mA)	± 100mA
Resolution (mA)	0.5 mA
Tolerance (%)	%4 for 10.85 A saturation
	%3 for 5.55 A saturation

Error value is calculated from the difference between current that passing through the core and the compensation current applied in reverse direction to the measured current. For the core saturated with 10.85A, the current applied to the conductor passing through the core with 10mA steps is illustrated in Fig. 5 and compensation current is illustrated in Fig. 6. For the core saturated with 5.55A, the current applied to the conductor passing through the core with 10mA steps is illustrated in Fig. 9 and compensation current is illustrated in Fig. 10. As it seems in TABLE II and TABLE III compensation current is nonlinear between 0 to 10 mA, noise is effective and it disturbs the compensation currents output. It became linear after 10 mA at each step's difference at harmonic is increased linearly. Performance parameters of the current sensor are given in TABLE IV.

V. CONCLUSION

In this work, an SRF method is proposed and implemented for DC measurements. The sense winding output signal is given to the TMS320F2837D's ADC channel. The graphed signals can be seen in Fig. 3 and Fig. 7 The calculated error value is given to the PI controller to generate a compensation current that cancel the magnetic flux. For the same magnitude measured current and

compensation current, magnetic flux changes back to the initial value. The sensor can measure the of current up to ±100mA and it can be increased in future works. Measurement ranges can be increased by shifting to the sensed signal to the ADC's limits. Sensor is sustainable since compensation current is applied to the system and difference at second harmonic is decreased to its zero-flux value.

In other studies, the triangle method and second harmonic demodulators were used for DC measurements. With the proposed SRF control method, the second harmonic demodulator has been applied to the system with an analysis of the park transformation via software and the response speed of the compensation current with the changes in the measured current is as much as the created closed-loop system response. Accuracy is up to 0.5mA and it can be increased by increasing the ADC's resolution also measured current ranges can be increased by ADC's upper limits. Applicability of the sensor is simple since it calculates the current by control algorithm electronic usage is reduces also another solution can be added and tested on the control algorithm without affecting the hardware.

As a result of the study, the proposed SRF method can detect the DC, and it stands out with its applicability, maintainability, and simplicity. For future works the sensed signal can be reduced to the ADC's limit so current measurement range can be increased, different types of cores can be used and noise should be decreased in order to get better resolution. AC measurement can be added to the sensor system with a new topology.

ACKNOWLEDGMENT

Emre DURNA, PhD, thanks for his contributions to this study and guidance in the testing process.

REFERENCES

[1] Calar, M., Durna, E., & Kayisli, K. (2022, March). 3-Phase Multi-Pulse Rectifiers with Different Phase Shifting Transformers and Comparison of Total Harmonic Distortion. In *2022 9th International Conference on Electrical and Electronics Engineering (ICEEE)* (pp. 60-64). IEEE.

[2] Xiao, C., Zhao, L., Asada, T., Odendaal, W. G., & Van Wyk, J. D. (2003, October). An overview of integratable current sensor technologies. In *38th IAS Annual Meeting on Conference Record of the Industry Applications Conference, 2003.* (Vol. 2, pp. 1251-1258). IEEE.

[3] Grim, V., Ripka, P., & Bauer, J. (2020). DC current sensor using switching-mode excited in-situ current transformer. *Journal of Magnetism and Magnetic Materials*, *500*, 166370.

[4] K Filanovsky, I. M., & Piskarev, V. A. (1991). Sensing and measurement of dc current using a transformer and RL-multivibrator. *IEEE transactions on circuits and systems*, *38*(11), 1366-1370.

[5] Castro, N., Reis, S., Silva, M. P., Correia, V., Lanceros-Mendez, S., & Martins, P. (2018). Development of a contactless DC current sensor with high linearity and sensitivity based on the magnetoelectric effect. *Smart Materials and Structures*, *27*(6), 065012.

[6] Ziegler, S., Borle, L. J., & Iu, H. H. C. (2008). Transformer-based DC current sensor for digitally controlled power supplies. *Australian Journal of Electrical and Electronics Engineering*, *5*(3), 245-253.

[7] Ripka, P., Draxler, K., & Styblikova, R. (2012). Measurement of DC currents in the power grid by current transformer. *IEEE transactions on magnetics*, *49*(1), 73-76.

[8] Kelley, A. W., & Titus, J. E. (1991, June). DC current sensor for PWM converters. In *PESC'91 Record 22nd Annual IEEE Power Electronics Specialists Conference* (pp. 641-650). IEEE.

[9] Azab, E., Hegazy, Y. G., Reeg, H., Schwickert, M., & Hofmann, K. (2021). Tunneling Magnetoresistance DC Current Transformer for Ion Beam Diagnostics. *Sensors*, *21*(9), 3043.

[10] Unser, K. (1969). Beam current transformer with DC to 200 MHz range (No. ISR-CO-69-6).

[11] Sonoda, T., Ueda, R., & Koga, K. (1992). An ac and dc current sensor of high accuracy. *IEEE transactions on industry applications*, *28*(5), 1087-1094.

[12] Unser, K. (1981). A toroidal DC beam current transformer with high resolution. *IEEE Transactions on Nuclear Science*, *28*(3), 2344-2346.

[13] Unser, K. B. (1985). Toroidal AC and DC current transformers for beam intensity measurements. *Atomkernenerg. Kerntech.*, *47*(CERN-LEP-BI-85-36), 48-52.

[14] Soliman, E., Hofmann, K., Reeg, H., & Schwickert, M. (2014). Sensor studies for DC current transformer application. *Proceedings of IBIC2014, Monterey, CA, USA*, 624-628.

[15] Aguilera, S., Odier, P.,s & Ruffieux, P. (2013). *Magnetic materials for current transformers* (No. CERN-ACC-2013-0303).

[16] Kesler, M., & Ozdemir, E. (2010). Synchronous-reference-frame-based control method for UPQC under unbalanced and distorted load conditions. *IEEE transactions on industrial electronics*, *58*(9), 3967-3975.

[17] Durna, E. (2018). Hysteresis band control of hybrid active power filter: An application to a medium-frequency induction melting furnace.